Supporting Information

Förster Resonance Energy Transfer between Colloidal $CuInS_2$/ZnS Quantum Dots and Dark Quenchers

*Chenghui Xia,[a] Wentao Wang,[b,§] Liang Du,[b] Freddy T. Rabouw,[a] Dave J. van den Heuvel,[a] Hans C. Gerritsen,[a] Hedi Mattoussi,[b] and Celso de Mello Donega[a]**

a. Debye Institute for Nanomaterials Science, Utrecht University, P.O. Box 80000, 3508 TA Utrecht, The Netherlands

b. Department of Chemistry and Biochemistry, Florida State University, Tallahassee, 32306 Florida, United States

*Corresponding author: E-mail: c.demello-donega@uu.nl

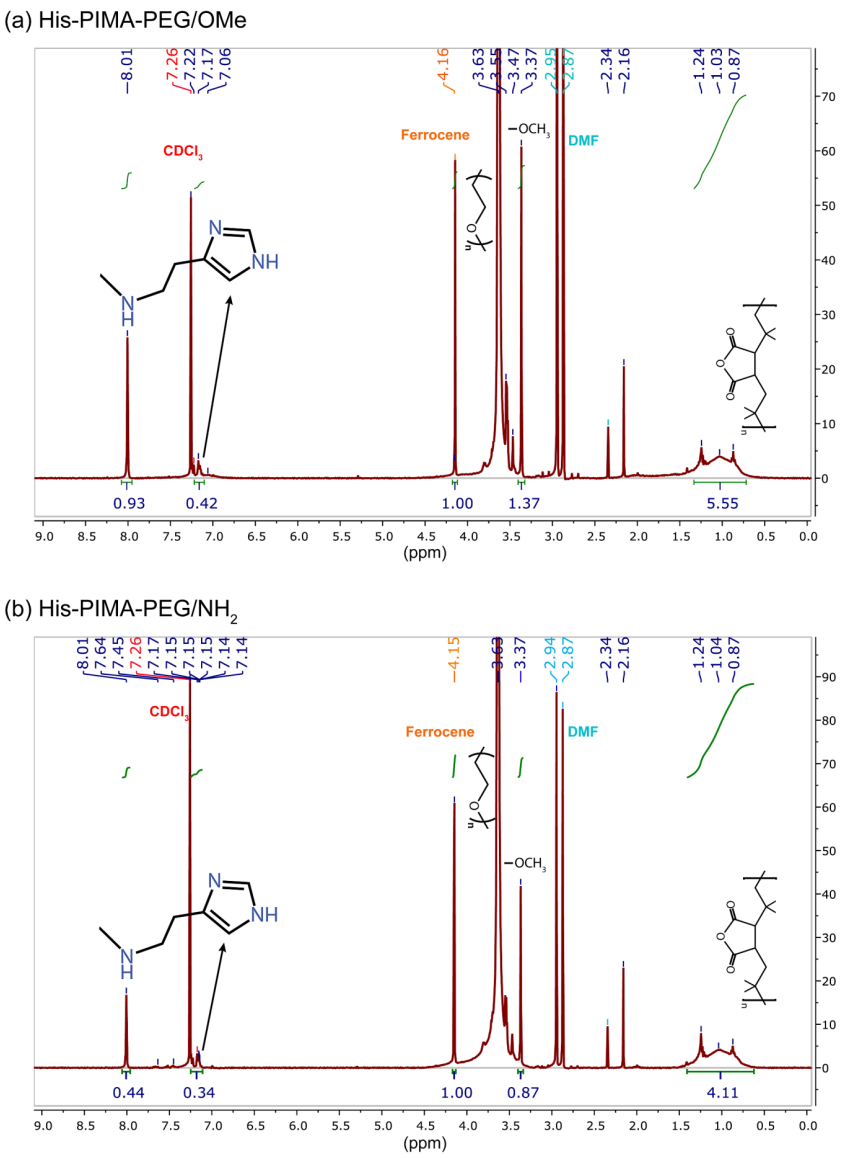

Figure S1. ^{1}H nuclear magnetic resonance (NMR) spectra of the product His-PIMA-PEG/OMe **(a)** and His-PIMA-PEG/NH_2 **(b)** polymer ligands. The resonances at ~7.15 ppm are ascribed to the protons from the imidazole rings. The strong signatures at 3.63 ppm and at 3.37 ppm are attributed to the resonances from the protons in the PEG segments and in the terminal methoxy groups, respectively. The peaks at 2.87 ppm and 2.94 ppm are from the protons of methyl groups in the residual N,N-Dimethylformamide (DMF) after synthesis. It should be noted that the proton from acyl group of DMF might also contribute to the resonance at 8.01 ppm. This peak therefore is not suitable for estimating the number of imidazole rings unless the DMF is completely removed. A broad peak at ~1.04 ppm is attributed to the protons of methyl groups in the PIMA backbone. The degree of grafting is estimated by comparing the signal integrations of the 3 protons from terminal methoxy group of the polyethylene glycol (PEG) segments (3.37 ppm), the proton from imidazole rings (7.14 ppm), and the protons from methyl groups of PIMA chains (~1.04 ppm). The results are shown in Figure 1b in the maintext. Deuterated chloroform ($CDCl_3$, 7.26 ppm) was used as the solvent. The purity was estimated using the information of grafting degree and known amount of ferrocene in $CDCl_3$ as a standard. The detailed calculation is listed below.

1) 14 mg product His-PIMA-PEG/OMe and 16 mg product His-PIMA-PEG/NH_2 polymer ligands were dissolved into 600 μL of $CDCl_3$ in the presence of 10.9 μL and 14.9 μL of 0.2 M ferrocene, respectively.

2) Estimation of the average molecular weight M_x using the NMR results in Figure S1 and Figure 1b. Since the number of NH_2-PEG-NH_2 groups could not be precisely determinated, the average molecular weight of His-PIMA-PEG/NH_2 was estimated by assuming 0, 1, 2, 3 NH_2-PEG-NH_2 groups per PIMA chain, respectively. Herein, two groups per chain were used as an example.

$M_{\text{His-PIMA-PEG/OMe}} = MW_{PIMA} + N_{His} \times MW_{His} + N_{NH2\text{-}PEG\text{-}OMe} \times MW_{NH2\text{-}PEG\text{-}OMe}$
$= (6000 + 18 \times 111.15 + 19 \times 753)$ g/mol$= 22307.7$ g/mol

$M_{\text{His-PIMA-PEG/NH2}} = MW_{PIMA} + N_{His} \times MW_{His} + N_{NH2\text{-}PEG\text{-}OMe} \times MW_{NH2\text{-}PEG\text{-}OMe} + N_{NH2\text{-}PEG\text{-}OMe} \times MW_{NH2\text{-}PEG\text{-}NH2} = (6000 + 19 \times 111.15 + 17 \times 753 + 2 \times 600)$ g/mol$= 22112.9$ g/mol

3) The gross amount n_{gross} of polymers then is,

$n_{\text{gross His-PIMA-PEG/OMe}} = m_{\text{His-PIMA-PEG/OMe}}/M_{\text{His-PIMA-PEG/OMe}} = 14 / 22307.7$ mmol$= 6.28 \times 10^{-4}$ mmol

$n_{\text{gross His-PIMA-PEG/NH2}} = m_{\text{His-PIMA-PEG/NH2}}/M_{\text{His-PIMA-PEG/NH2}} = 16 / 22112.9$ mmol$= 7.24 \times 10^{-4}$ mmol

4) The net amount n_{net} of polymers can be obtained from NMR results,

$n_{\text{net His-PIMA-PEG/OMe}} = 5.17 \times 10^{-4}$ mmol

$n_{\text{net His-PIMA-PEG/NH2}} = 5.23 \times 10^{-4}$ mmol

5) Therefore, the purity η of polymer ligands is,

$\eta_{\text{His-PIMA-PEG/OMe}} = n_{\text{net His-PIMA-PEG/OMe}} / n_{\text{His-PIMA-PEG/OMe}} = 82.3\%$

$\eta_{\text{His-PIMA-PEG/NH2}} = n_{\text{net His-PIMA-PEG/NH2}} / n_{\text{His-PIMA-PEG/NH2}} = 72.2\%$

Remarks: The purity of His-PIMA-PEG/NH_2 was averaged by redoing the calculation but changing the number of NH_2-PEG-NH_2 groups ($\eta_0 = 68.4\%$, $\eta_1 = 70.3\%$, $\eta_2 = 72.2\%$, $\eta_3 = 74.3\%$). In this case, the average purity of His-PIMA-PEG/NH_2 was ~71%.

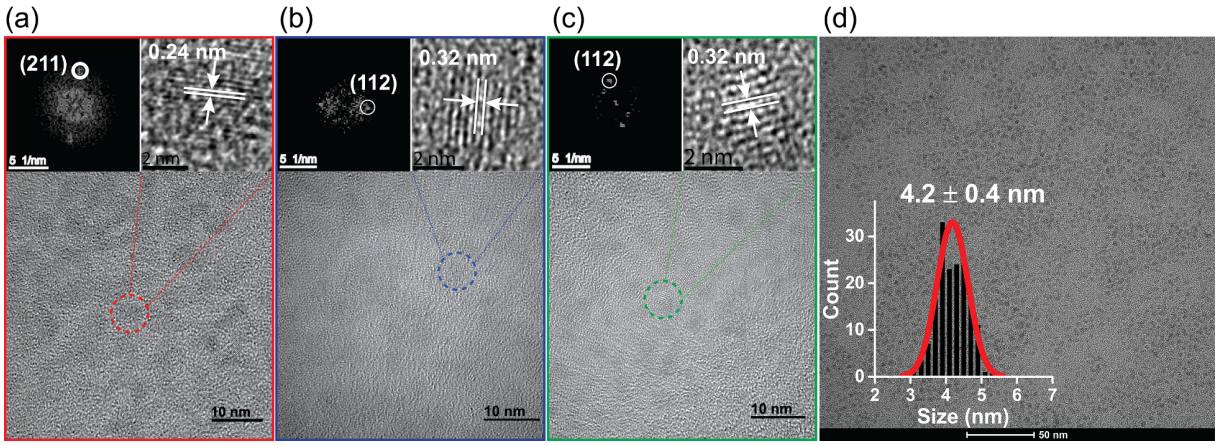

Figure S2. (a-c) HRTEM, corresponding Fourier transform (FT) analysis, and inverse FT images of bare $CuInS_2$ cores (a), gradient-alloy $(Cu,In,Zn)S_2$ QDs (b) and $CuInS_2$/ZnS core/shell QDs (c). FT patterns are acquired from the area of interest indicated by red box. The lattice spacings in a, b and c are 2.4, 3.2 and 3.2 Å, which correspond well to the {211}, {112} and {112} lattice planes of the chalcopyrite $CuInS_2$, respectively. **(d)** Zoom out TEM image of $CuInS_2$/ZnS core/shell QDs in c. The inserted size histogram was constructed by measuring the diameter (4.2 nm with a polydispersity of 9.5%) of over 200 QDs and was fitted to a Gaussian distribution function.

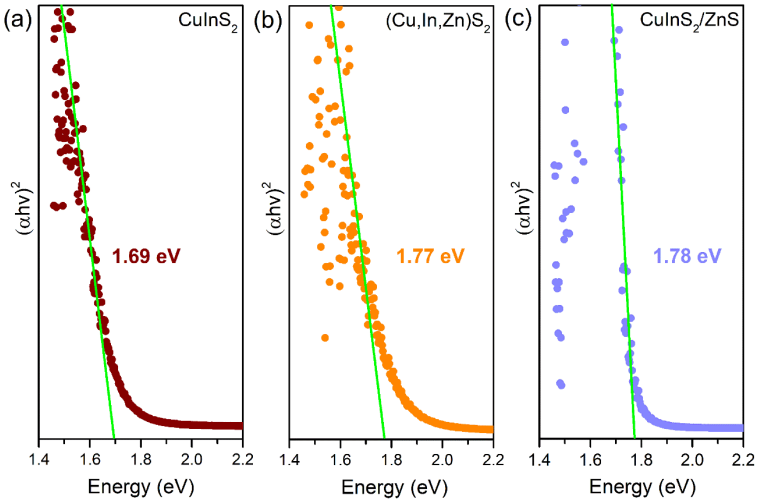

Figure S3. Experimental band gap estimation of $CuInS_2$ cores **(a)**, gradient-alloy $(Cu,In,Zn)S_2$ QDs **(b)**, and $CuInS_2$/ZnS core/shell QDs **(c)** using a Tauc plot. A pronounced blue-shift (80 meV) is observed after the first step of ZnS shelling, while a slight blue-shift (10 meV) is found after the second step of ZnS shelling. The band gaps of product QDs (direct band-gap semiconductors) were calculated by Tauc plot according to $(ahv)^2 = [hv \times (1-Abs)^2/2Abs]^2$ (Lu, X. *et al.*, *Chem. Commun.* **2011**, *47*, 3141−3143).

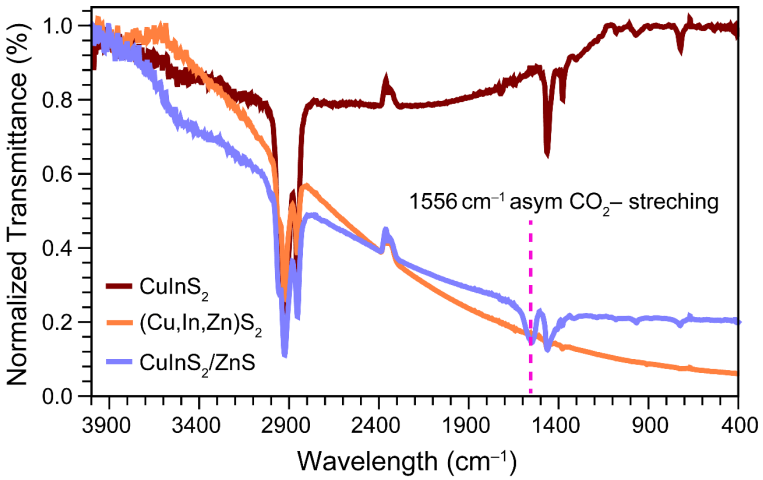

Figure S4. FTIR spectra of bare $CuInS_2$ QDs, gradient-alloy $(Cu,In,Zn)S_2$ QDs and $CuInS_2/ZnS$ core/shell QDs. The peak at 1556 cm^{-1} in the spectrum of the product $CuInS_2/ZnS$ QDs after SILAR reaction is assigned to asymmetric C(=O)O– stretching of carboxylic acid group from $Zn(oleate)_2$.

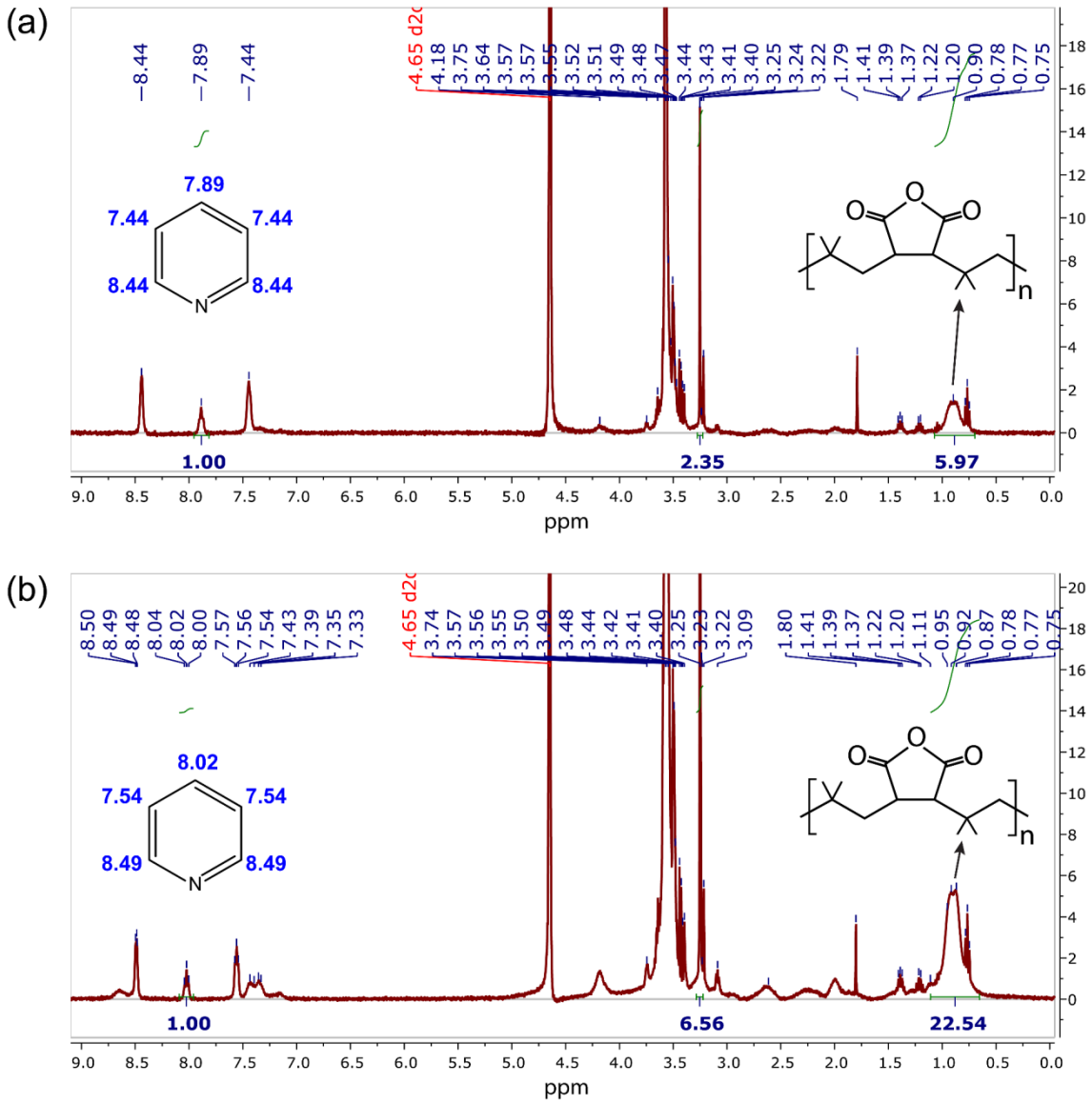

Figure S5. ^{1}H NMR spectra of QDs-OMe **(a)** and QDs-NH_2 **(b)** mixed with a certain amount of pyridine. The resonances at ~8.4 ppm, ~7.9 ppm and ~7.5 ppm are attributed to the protons from pyridine while a broad resonances at ~0.9 ppm are ascribed to the protons of methyl groups in the PIMA backbone. The ligand density was estimated by comparing the molar concentrations of the polymer ligands and that of the $CuInS_2$/ZnS QDs in the medium. The concentration of polymer ligands can be obtained by comparing the integrations of the methyl-protons of the PIMA backbone and γ-proton of the pyridine standard. Deuterated oxide (D_2O) was used as the solvent.

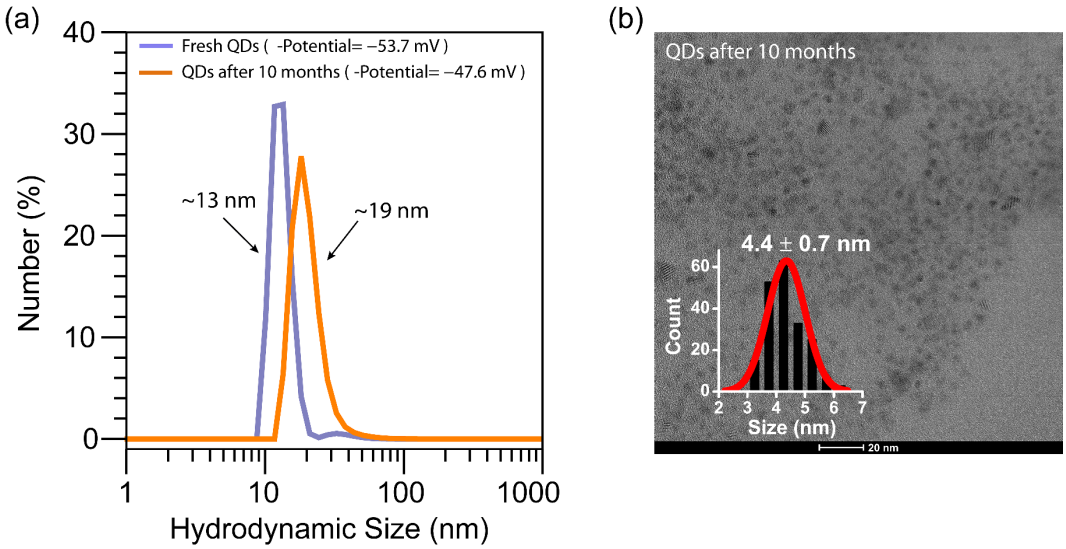

Figure S6. (a) The hydrodynamic diameter of fresh QDs-NH_2 and the QDs-NH_2 after storage at 4 °C for 10 months. The zeta potential value is obtained during the measurements. The pH values of the fresh QDs and the QDs after 10-month storage are 6.4±0.1 and 5.9±0.2, respectively. All these measurements were obtained at room temperature (20 °C). (b) TEM image and corresponding size distribution histogram of QDs-NH_2 after storage at 4 °C for 10 months. The inserted size histogram was constructed by measuring the diameter of over 200 QDs and was fitted to a Gaussian distribution function.

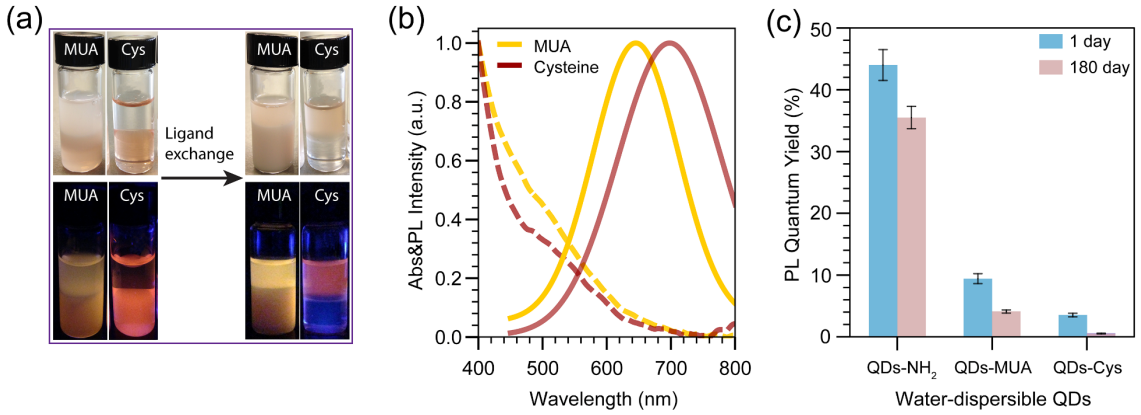

Figure S7. (a) Digital images of ligand exchange process using 11-mercaptoundecanoic acid (MUA) and cysteine (Cys). The upper panels are $CuInS_2$/ZnS QD solutions under natural light while the bottom panels are those under 365 nm UV-lamp. The upper layer is water while the bottom layer is chloroform. The ligand exchange was performed following previously reported procedures (Xia, C. *et al.*, *Chem. Mater.* **2017**, *29*, 4940–4951). **(b)** Absorption and PL spectra of MUA and Cys capped $CuInS_2$/ZnS QDs. **(c)** Histogram plots of PL quantum yields (QYs) of His-PIMA-PEG/NH_2, MUA, and Cys capped $CuInS_2$/ZnS QDs before and after 180-day storage in dark at 4 °C, respectively. The QD concentrations of these water-dispersible QDs were kept nearly the same (~10 μM) for the long-term stability test.

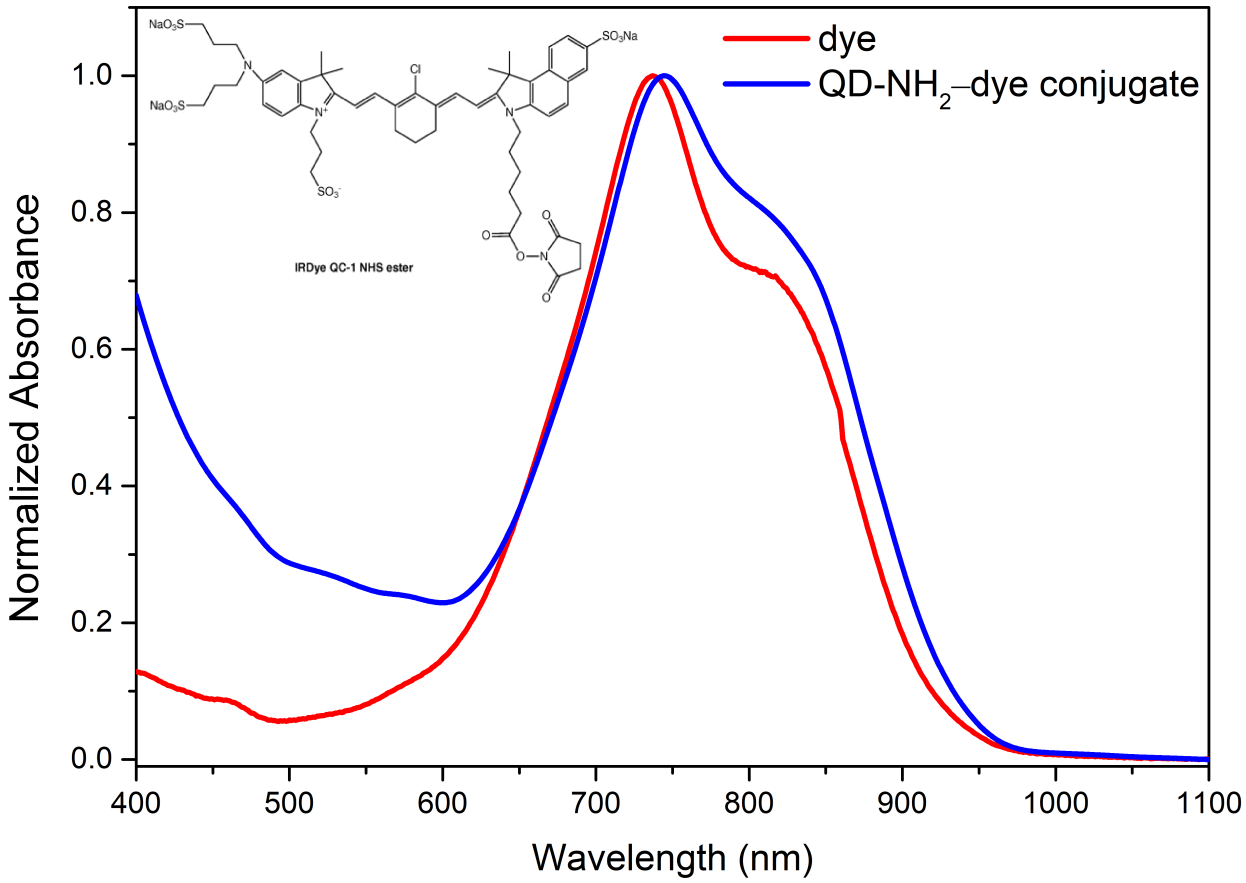

Figure S8. (a) Normalized absorption spectra of IRDye QC-1 dark quencher in 1×PBS solution (red line) and QD-NH_2-dye conjugates in deionized water (blue line). Inset is the dye molecular structure. Slight red shift of absorption spectrum of QD-NH_2-dye conjugates may be due to dimerization.

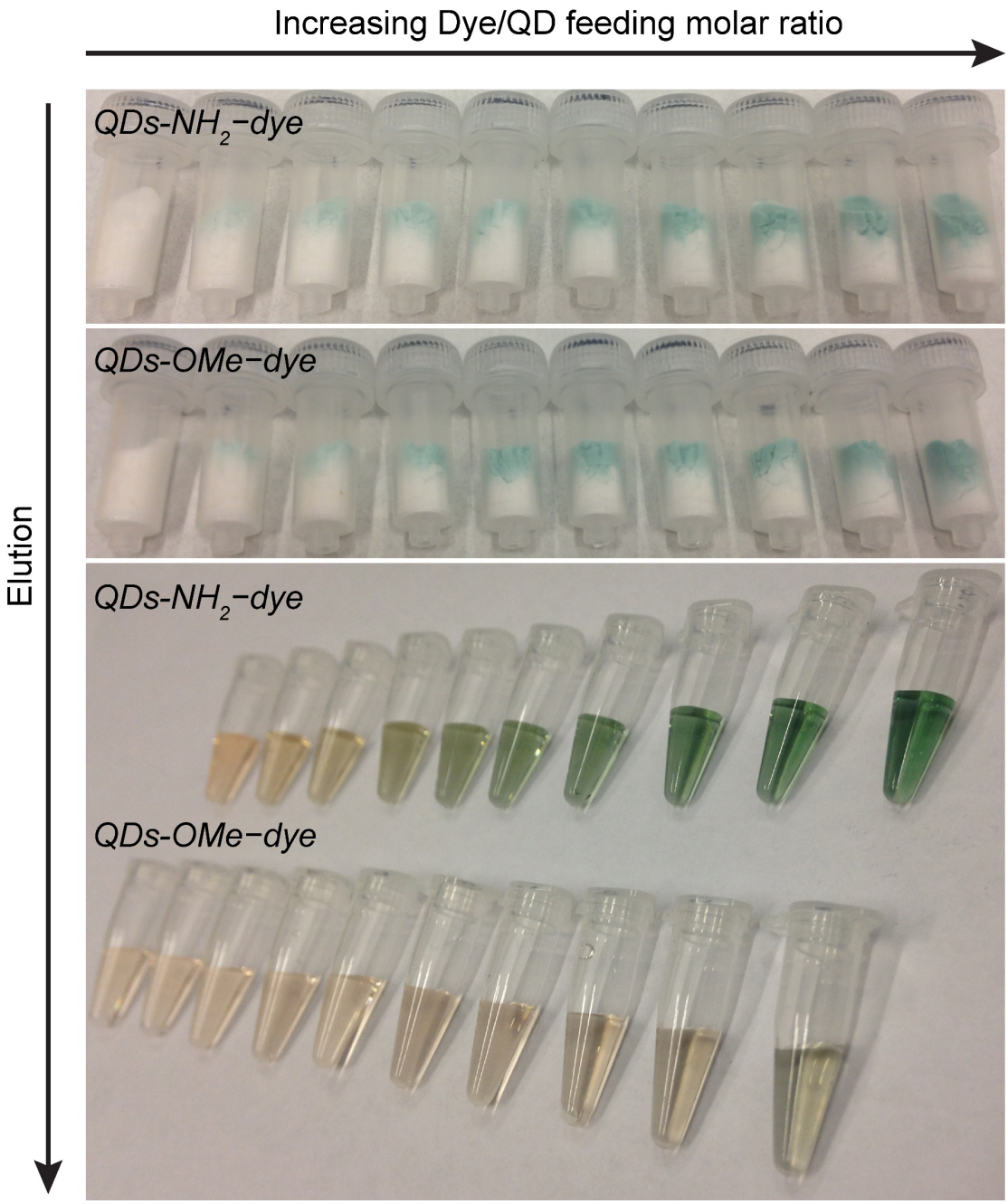

Figure S9. The upper panel shows digital images of the used G-25 columns after the separation by size-exclusion chromatography. The lower panel shows digital images of colloidal dispersions of the product QDs-OMe−dye and QDs-NH_2−dye conjugates in water. The QD-dye conjugates are ordered according to the dye/QD feeding molar ratios from 0 to 20 (increasing from left to right).

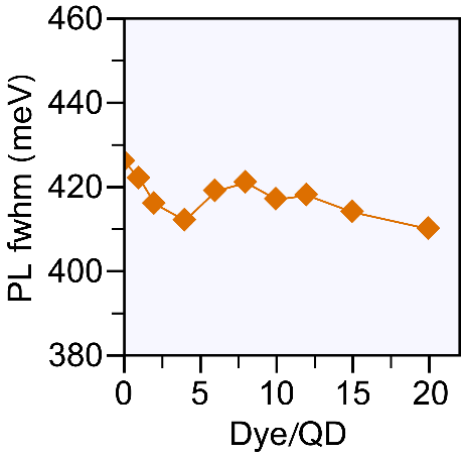

Figure S10. Full width at half maximum (fwhm) of the PL bands shown in Figure 5f upon increasing the amount of dark quencher dye molecules attached to QDs.

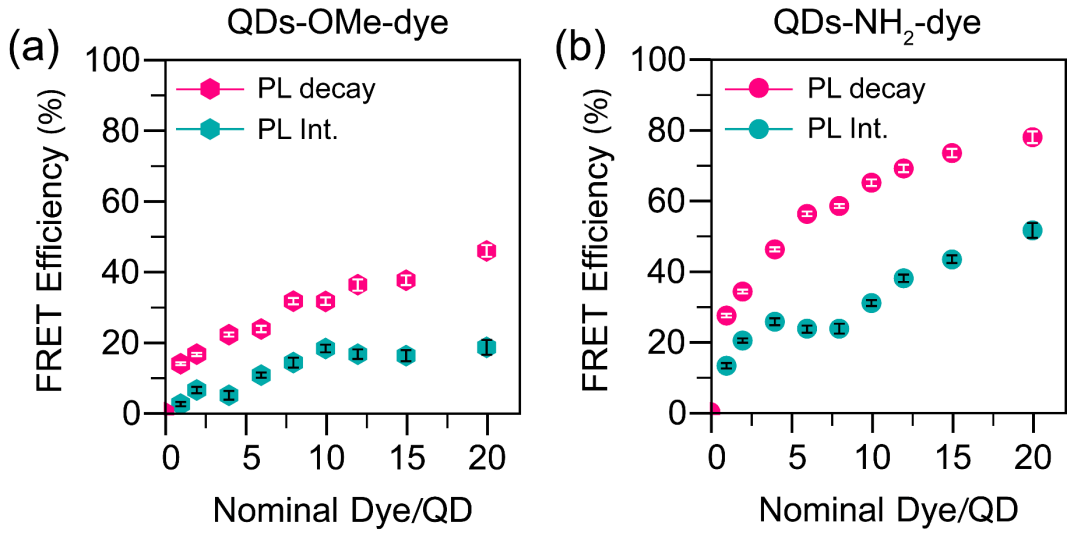

Figure S11. Overall FRET efficiency of **(a)** QDs-OMe–dye and **(b)** QDs-NH_2–dye conjugates upon increasing the amount of dark quencher dye molecules conjugated to the QD donors. Note that the nominal Dye/QD feeding ratio is used instead of the actual Dye/QD ratio. The FRET efficiencies were obtained from the PL quenching data (green) or from the shortening of the exciton lifetimes of the QDs (pink) using eq. 1 in the main text. The error bars are generated from integration errors of PL decay and PL spectra.

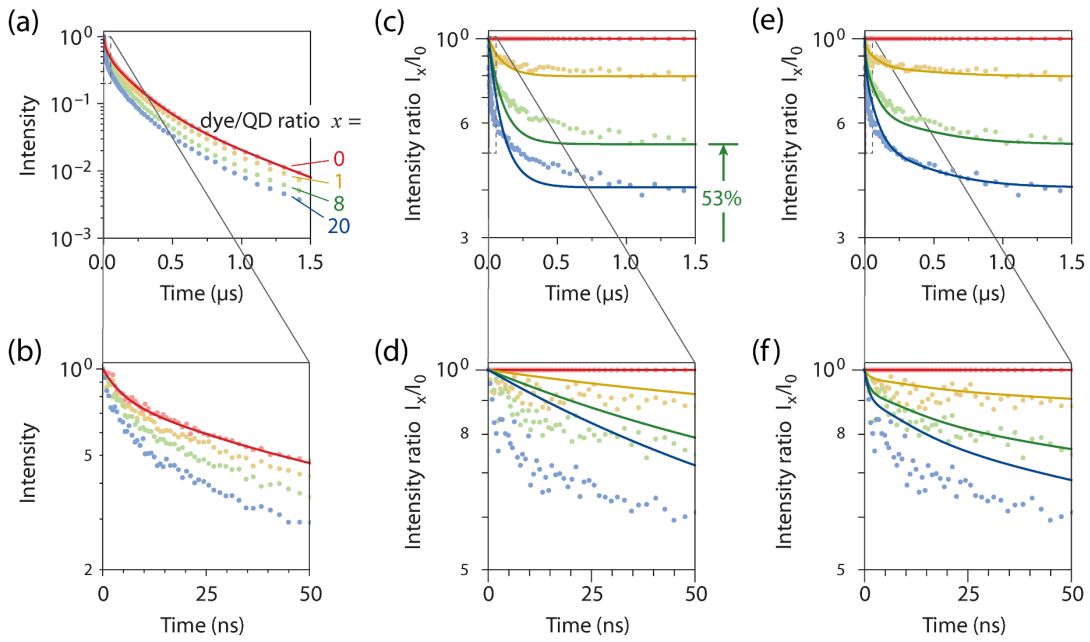

Figure S12. (a-b) Examples of PL decay curves of QDs-OMe−dye conjugates at different nominal dye/QD ratios x = 0 (red), 1 (yellow), 8 (green), 20 (blue). Logarithmic binning was used for the PL decay curves to improve the signal-to-noise ratio at long times. A four-exponential decay function $[A_1e^{-t/\tau_1} + A_2e^{-t/\tau_2} + A_3e^{-t/\tau_3} + A_4e^{-t/\tau_4}]$ is used to describe the PL decay to the data without dye molecules (solid red lines), without giving any particular interpretation to the four exponents. b is a zoom of a. **(c-f)** The PL decay curves at dye/QD ratio x divided by the reference curve at x = 0. d and f are zooms of c and e. Four-exponential decay functions (solid lines) are used to describe the decays at different dye/QD feeding ratios, either considering the variations in non-radiative decay rates (model 1, c,d) or in radiative decay rates (model 2, e,f).

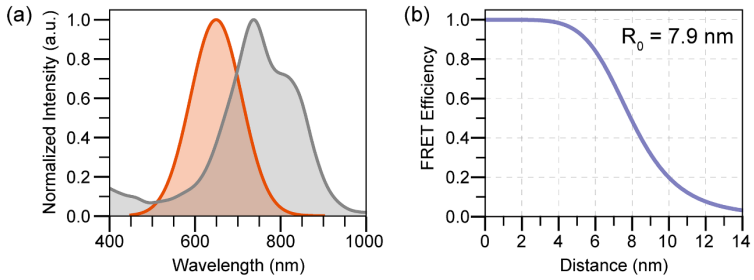

Figure S13. (a) Normalized emission spectrum of QDs-NH_2 (orange line) and absorption spectrum of IRDye QC-1 dark quencher dye molecules (grey line). The overlap integral (1.62×10^{18} $M^{-1}cm^{-1}nm^4$) was calculated by $J = \int \overline{I_D}\varepsilon_A\lambda^4 d\lambda$. **(b)** A plot of the distance-dependent FRET efficiency in a QDs-NH_2−dye donor−acceptor pair. The Förster distance R_0 is 7.9 nm.